*Biochimica et Biophysica Acta*, 688 (1982) 505–514
Elsevier Biomedical Press



BBA 71190

# THE HYPOXANTHINE TRANSPORTER OF NOVIKOFF RAT HEPATOMA CELLS EXHIBITS DIRECTIONAL SYMMETRY AND EQUAL MOBILITY WHEN EMPTY OR SUBSTRATE-LOADED

PETER G.W. PLAGEMANN and ROBERT M. WOHLHUETER

*Department of Microbiology, Medical School, University of Minnesota, Minneapolis, MN 55455 (U.S.A.)*

(Received November 23rd, 1981)

*Key words: Hypoxanthine transporter; Directional symmetry; Mobility; (Novikoff hepatoma cell)*

**The kinetics of hypoxanthine transport were measured in hypoxanthine phosphoribosyltransferase-deficient Novikoff cells by rapid kinetic techniques applying both zero-*trans* and equilibrium exchange protocols. The data indicate operation of a simple carrier with directional symmetry and equal mobility when substrate loaded and empty. Zero-*trans* influx and efflux were about equivalent and so were zero-*trans* influx and equilibrium exchange flux. The apparent Michaelis-Menten constant and maximum velocity were about 500 $\mu$M and 100 pmol/s per $\mu$l cell $H_2O$, respectively. The time courses of accumulation of radioactively labeled hypoxanthine at a concentration above the Michaelis-Menten constant differed noticeably in zero-*trans* and equilibrium exchange mode, but computer simulations showed that the difference is predicted by the symmetrical carrier model and does not reflect *trans*-stimulation.**

## Introduction

In a previous study [1] we have measured the zero-*trans* * influx of hypoxanthine in various types of cultured cells, but in greatest detail in Novikoff rat hepatoma cells, in which its conversion to nucleotides was blocked because the cells were depleted of ATP and *P*-Rib-*PP*, or deficient in hypoxanthine-guanine phosphoribosyltransferase (EC 2.4.2.8), or both. Hypoxanthine transport is very rapid in these cells; the half-time ($t_{1/2}$) for transmembrane equilibration in the first-order range of substrate concentration is 4 to 12 s, which is at least 50-times more rapid than the non-mediated permeation of hypoxanthine through the plasma membrane at these concentrations [1,3]. In this paper, 'transport' denotes solely the transfer of unmodified exogenous substrate across the cell membrane as mediated by a saturable, selective carrier.'Uptake' denotes the transfer of radioactivity from exogenous labeled substrate to intracellular space or components regardless of metabolic conversions. Because the initial linear phase of substrate accumulation is too short to allow accurate, graphical estimation of initial transport velocities, we have resorted to fitting an integrated rate equation (Eqn. I, Materials and methods) based on a simple carrier model [2] to complete time courses of substrate accumulation to transmembrane equilibrium. This approach not only allows estimation of true initial velocities, but also the evaluation of various transport models. The equation used in

* As defined by Eilam and Stein [2], 'zero-*trans*' designates the transport of a substrate from one side of the membrane to the other side, where its concentration is zero. 'Equilibrium exchange' designates the unidirectional flux of radioactively labeled substrate from one side to the other side of the membrane, where substrate is held at equal concentration. Arbitrarily, we designate the outside and inside faces of the membrane as 1 and 2, respectively.

0005-2736/82/0000–0000/$02.75 © 1982 Elsevier Biomedical Press

these analyses assumes symmetry of the transporter with respect to direction and equality of mobility of loaded and empty carrier. Carrier 'mobility' denotes some macromolecular movement, if only a conformational shift, and not necessarily carrier translocation. These assumptions reduce the number of parameters to be fit to two ($K$ and $V$) which is necessary for successful regression of the zero-*trans* equation on the sets of data supplied by our experimental protocols (6–8 substrate concentrations, 15 time points per substrate concentration, see Ref. 4). The excellent fit of Eqn. I to our experimental data seemed to justify this approach and suggested the operation of a symmetrical carrier whose mobility is the same whether empty or loaded with hypoxanthine. Kinetic analyses of four independent zero-*trans* entry experiments yielded a mean Michaelis-Menten constant for hypoxanthine transport in Novikoff cells of $349 \pm 17$ $\mu$M and a mean maximum velocity of $53 \pm 10$ pmol/s per cell $H_2O$ [1,3]. Similar values were obtained for other cell lines [3]. In the present study we have expanded our previous studies to compare zero-*trans* influx and efflux and inward and outward equilibrium exchange of hypoxanthine in hypoxanthine-guanine phosphoribosyltransferase-deficient Novikoff cells and thereby obtained direct evidence for the directional symmetry of the hypoxanthine carrier and its equal mobility whether or not it is loaded with hypoxanthine.

## Materials and Methods

*Cell culture.* Novikoff rat hepatoma cells and an 8-azaguanine-resistant mutant thereof (subline 1–9) lacking hypoxanthine-guanine phosphoribosyltransferase [5] were propagated in suspension culture in Swim's medium 67 as previously described [6], except that the medium and its preparation has been modified. The medium has been supplemented with 200 mg sodium succinate and 15 mg succinic acid per liter to permit sterilization of the basal medium by autoclaving (Swim, H.E., personal communication). The appropriate amount of premixed S-210 powder (GIBCO) was dissolved in 9740 ml of distilled water and supplemented with 10.6 g Pluronic F68 [6]. This basal medium was autoclaved at 121°C for 90 min, and, after cooling, was supplemented aseptically with 250 ml filter-sterilized 8.14% (w/v) $NaHCO_3$, 10 ml of a filter-sterilized solution of 62.5 mg penicillin G and 12.5 mg streptomycin sulfate per ml of water, 500 ml sterile calf serum and 500 ml of a filter-sterilized 10% (w/v) solution of Primatone-RL (Humko Sheffield Chemical, White Station Tower, TN). Cells were enumerated with a Coulter electronic counter and cell viability was assessed by staining with Trypan blue. Cultures were examined for mycoplasma by the uracil/uridine incorporation method [7] and cultural techniques [8]. No mycoplasma contamination was detected.

*Transport measurements.* Cells were harvested from late exponential phase cultures and suspended in basal medium 42B [9]. The accumulation of radioactively labeled hypoxanthine was measured at 25°C by a rapid mixing/sampling method described in detail previously [10,11]. The method consists of mixing cell suspension at $(2–3) \cdot 10^7$ cells/ml with a solution of radioactively labeled substrate in short intervals with a dual syringe apparatus (5 ml and 1 ml syringe) in a ratio of 7.4:1. The cells are separated from the medium by centrifugation through oil and analyzed for radioactivity. Radioactivity per cell pellet was corrected for that attributable to extracellular space and converted to pmol/$\mu$l cell water.

For zero-*trans* influx measurements, the initial intracellular concentration of hypoxanthine was assumed to be negligible. For inward equilibrium exchange measurements, samples of cell suspension were supplemented with specified concentrations of unlabeled hypoxanthine, incubated at 37°C sufficiently long to ensure transmembrane equilibrium (about 15 min) and, after cooling at 25°C, the accumulation of radioactively labeled hypoxanthine at the preloading concentration was measured as described above. In both cases an increasing cell content of radioactivity was measured.

For measurements of efflux of radioactively labeled hypoxanthine, samples of suspension of $(1–2) \cdot 10^8$ cells/ml were equilibrated with specified concentrations of radioactively labeled hypoxanthine. Then a suspension of preloaded cells was mixed at timed intervals in a ratio of 1:7.4 (opposite to that in influx measurements) with basal medium devoid of substrate (exit) or of basal

medium containing unlabeled hypoxanthine at the same concentration as labeled hypoxanthine used for preloading the cells (outward equilibrium exchange). The cells were separated from the medium by centrifugation through oil and analyzed for radioactivity as in the influx protocol. In this case a decreasing cellular content of radioactivity was measured. Exit measurements with this protocol are not strictly 'zero-*trans*', since the extracellular concentration of substrate at zero-time is not nil, but rather 12% that inside the cells.

For an analysis of the labeled components in the acid-soluble pool, labeled cells were centrifuged through oil directly into an underlying acid solution which was analyzed chromatographically as described previously [1].

*Treatment of the data.* We generally follow the nomenclature and definitions of kinetic parameters formulated by Eilam and Stein [2]. We have integrated over time the flux equations developed by these investigators for the simple carrier model [10,11]. For a carrier with directional symmetry and equal mobility whether empty or loaded the zero-*trans* entry equation reduces to:

$$S_{2,t} = S_1\left(1 - \exp\left(-\frac{tV + (1 + S_1/K)S_{2,t}}{K + 2S_1 + S_1^2/K}\right)\right) \quad (1)$$

where $S_{2,t}$ = concentration of intracellular substrate at time $t$ ($S_{2,0} = 0$); $S_1$ = extracellular concentration of substrate (and is taken as a constant); $K$ = Michaelis-Menten constant, and $V$ = maximum velocity.

The time course of isotopic exchange at equilibrium is given by:

$$N_{2,t} = N_{2,\infty}\left(1 - \exp\left(-\frac{V^{ee}t}{K^{ee} + S}\right)\right) \quad (2)$$

for inward exchange and:

$$N_{2,t} = (N_{2,0} - N_{2,\infty})\left(\exp\left(-\frac{V^{ee}t}{K^{ee} + S}\right)\right) + N_{2,\infty} + N_{2,x} \quad (3)$$

for outward exchange, where $N_{2,t}$ = intracellular concentration of radioactivity at time $t$; $S$ = substrate concentration which is equal on both sides of the membrane, and $K^{ee}$ and $V^{ee}$ are the apparent Michaelis-Menten constant and maximum velocity for equilibrium exchange, respectively. For inward exchange, $N_{2,\infty} = N_1$, the concentration of radioactivity per equivalent volume of medium. For outward exchange, $N_{2,\infty} = N_{2,0}/8.31$, and not zero, because of the carryover of radioactivity from the preloading mixture into the extracellular compartment which our procedure entails. In Eqn. 3, $N_{2,x}$ = non-effluxable radioactivity present intracellularly after preloading, which, in the case of hypoxanthine uptake by 1–9 cells, reflected small amounts of hypoxanthine converted to nucleotides during prolonged preincubation by means of residual hypoxanthine-guanine phosphoribosyltransferase activity in this mutant. $N_{2,x}$ was generally $< 20\%$ of $N_{2,0}$ (see Fig. 1). To facilitate comparison with net flux data, $N_2$ has been expressed as chemical concentration of radioactively labeled substrate at its initial specific radioactivity.

Eqns. 1–3 were fitted by a non-linear least-squares regression program based on the algorithm of Dietrich and Rothmann [12] to the appropriate time courses of substrate transmembrane equilibration pooled for seven substrate concentrations. Data were weighted as the reciprocal of substrate concentration, which, in effect, gives equal weighting with respect to amount of radioactivity. Convergence is defined as a change of $< 0.01\%$ in all parameter values on successive iterations. The program generates best fitting values of the kinetic parameters, the associated standard errors of estimate, the correlation coefficient ($r_{y,\hat{y}}$) of measured values of the dependent variable ($y$) on computed values ($\hat{y}$), and several plots depicting the individual residuals ($y - \hat{y}$) vs. the computed values, the independent variables ($S$ and $t$) and as an error distribution on a normal grid (Ref. 13; see for example, Fig. 4).

Initial zero-*trans* ($v_{12}^{zt}$) and equilibrium exchange ($v^{ee}$) velocities were calculated for a given substrate concentration as the slopes of the curves described by Eqns. 1 and 2 or 3, respectively, at $t = 0$: $v_{12}^{zt} = S_1V/(K + S_1)$ and $v^{ee} = SV^{ee}/(K^{ee} + S)$.

We have so far not been able to apply integrated rate analysis satisfactorily to time-courses of zero-*trans* exit of hypoxanthine. One problem is

the presence of non-effluxable radioactivity in preloaded cells, referred to already, which introduces an additional parameter to be fitted. However, for concentration of substrate well below the Michaelis-Menten constant for transport, the zero-*trans* rate equation for exit can be approximated by Eqn. 4, which is formally identical to Eqn. 3:

$$S_{2,t} = (S_{2,0} - S_{2,\infty})[\exp(-k't)] + S_{2,\infty} + S_{2,x} \quad (4)$$

where $k'$ = the apparent first-order rate constant $V/K$ and $S_{2,x}$ is a corrective term equivalent to $N_{2,x}$ in Eqn. 3. For concentrations of hypoxanthine $\ll K$ (i.e. 20 $\mu$M, see Fig. 1) we have estimated $v_{12}^{zt}$ by fitting Eqn. 4 to time-courses of substrate release. For concentrations of hypoxanthine $> K$ this approach is not applicable, so exit curves were drawn by hand.

*Materials.* [2-$^3$H]Hypoxanthine and [8-$^{14}$C]hypoxanthine were purchased from Moravek Biochemicals (Brea, CA) and diluted to the desired specific radioactivities with unlabeled hypoxanthine obtained from Sigma Chemical Co. (St. Louis, MO).

## Results and Discussion

*Hypoxanthine transport in hypoxanthine-guanine phosphoribosyltransferase-deficient cells*

Fig. 1 illustrates early time-courses of zero-*trans* entry and exit and inwards and outwards equilibrium exchange of hypoxanthine at concentrations of 20 $\mu$M and 2 mM in Novikoff rat hepatoma cells lacking hypoxanthine-guanine phosphoribosyltransferase. Chromatographic analysis of the

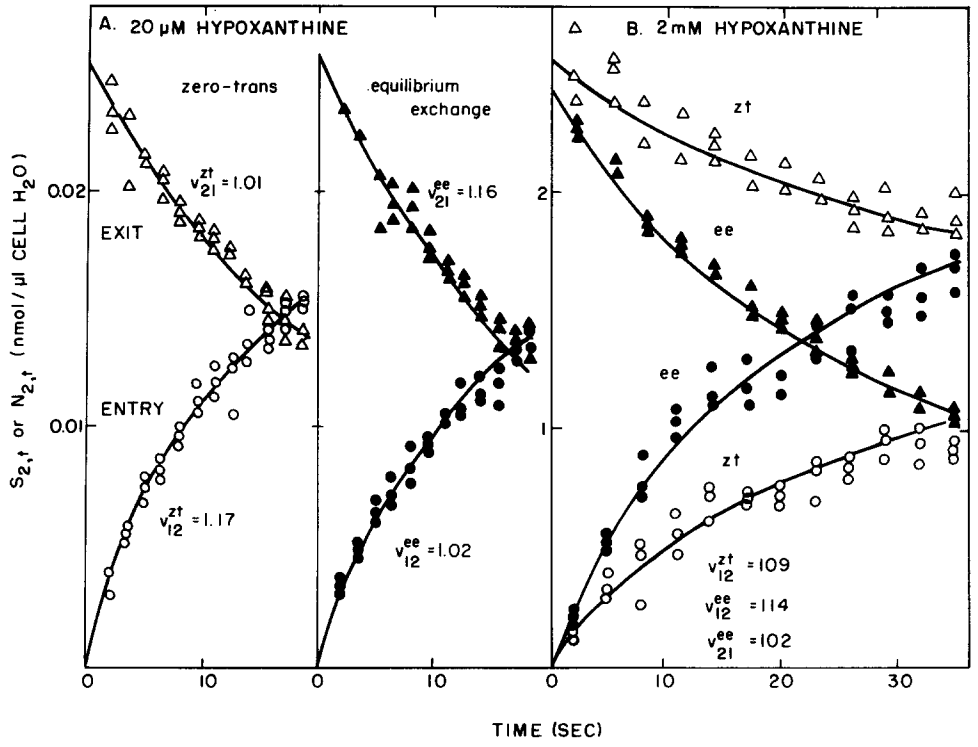


Fig. 1. Comparisons of initial time course of zero-*trans* entry and exit and inward and outward equilibrium exchange in hypoxanthine-guanine phosphoribosyltransferase-deficient Novikoff cells at 25°C. Changes in intracellular concentration of [$^{14}$C]hypoxanthine ($S_{2,t}$ or $N_{2,t}$) were measured in triplicate in four experimental protocols in the same population using the rapid kinetic technique. The concentration of radioactivity was 180 cpm/$\mu$l, regardless of the hypoxanthine concentration. Equations 1, 2 and 3 were fitted to the data for zero-*trans* entry (○———○), and inward (●———●) and outward (▲———▲) equilibrium exchange, respectively, with $K(=K^{ee})$ fixed at 450 $\mu$M. The listed initial zero-*trans* and equilibrium exchange velocities ($v_{12}^{zt}$ and $v^{ee}$ in pmol/s per $\mu$l cell $H_2O$) were calculated for $S_1 = S = 20$ $\mu$M or 2 mM by substituting the estimated values for $V$ and $V^{ee}$ into: $v_{12}^{zt} = S_1V/(K + S_1)$ and $v^{ee} = SV^{ee}/(K^{ee} + S)$, respectively. $v_{21}^{zt}(= k'S_{2,0})$ for 20 $\mu$M hypoxanthine was estimated by fitting Equation 4 to the zero-*trans* exit (△———△) data. The curve for zero-*trans* exit of hypoxanthine at 2 mM was drawn by hand.

acid-soluble pools of cells incubated with [$^3$H]hypoxanthine for 60 s showed that no significant phosphoribosylation had occurred during this time period. Directional symmetry of the hypoxanthine transporter is indicated by the approximate equivalence of the initial velocities of zero-*trans* entry ($v_{21}^{zt}$) (Fig. 1). Even though we can provide an accurate estimate for zero-*trans* exit only for 20 $\mu$M hypoxanthine (i.e., at $S \ll K$; see Materials and Methods), it is apparent that the entry and exit curves for 2 mM hypoxanthine also mirror one another fairly closely, i.e. that there was no gross difference in flux with respect to direction. Similarly comparable zero-*trans* exit and entry time-courses were observed in four other experiments with hypoxanthine concentrations ranging from 20 to 2000 $\mu$M.

Equivalent mobility of empty and hypoxanthine-loaded carrier is indicated by the approximate equality between initial velocities of zero-*trans* entry and exit ($v^{zt}$) and equilibrium exchange ($v^{ee}$) at a hypoxanthine concentration (2 mM in Fig. 1B) well above the Michaelis-Menten constant for hypoxanthine transport ($K$; see be-

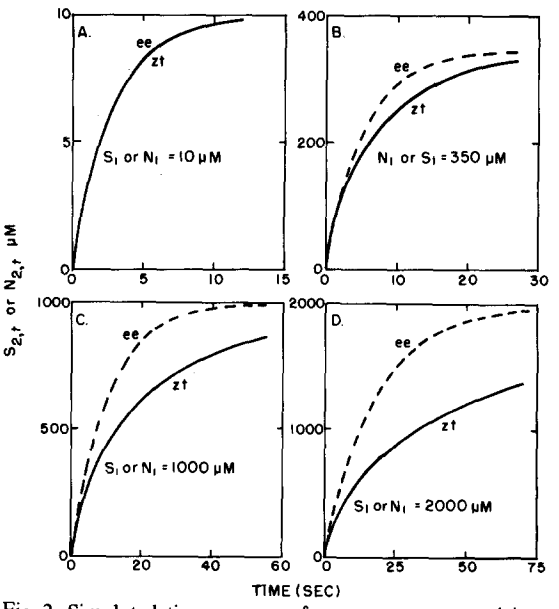


Fig. 2. Simulated time courses of zero-*trans* entry and inward equilibrium exchange for a simple transporter with directional symmetry and equal mobility when substrate loaded and empty. The progress curves for $S_{2,t}$ and $N_{2,t}$ were generated for the indicated substrate concentrations ($S_1$ or $N_1$) by numerical solution of Eqns. 1 and 2, respectively, with $K = K^{ee} = 450\mu$M and $V = V^{ee} = 130\ \mu$M/s.

TABLE 1

KINETIC CONSTANTS FOR ZERO-*TRANS* ENTRY (1→2) AND INWARD (1→2) AND OUTWARD (2→1) EQUILIBRIUM EXCHANGE OF HYPOXANTHINE IN HYPOXANTHINE-GUANINE PHOSPHORIBOSYLTRANSFERASE-DEFICIENT NOVIKOFF CELLS

The [$^3$H]hypoxanthine concentrations were generally 40, 80, 160, 320, 640, 1280, and 2560 $\mu$M (between 500 and 900 cpm/$\mu$l, regardless of concentration in individual experiments). The intracellular and extracellular $H_2O$ spaces fell between 15 and 20 $\mu$l and 2 and 4 $\mu$l per sample, respectively. The appropriate integrated rate equations (1–3) were fitted to the pooled data and the best fitting parameters are listed. Where indicated zero-*trans* entry and inward equilibrium exchange were measured in the same population of cells. Representative time courses of inward and outward equilibrium exchange from experiments 1 and 9, respectively, are illustrated in Fig. 3. Analyses of the residuals of the least-squares fits of the appropriate rate equations to the data from experiments 1 and 9 by a number of statistical procedures are illustrated in Fig. 4.

| Direction | Expt. | Zero-*trans* | | | Equilibrium exchange | | |
|---|---|---|---|---|---|---|---|
| | | $K$ ($\mu$M) | $V$ (pmol/s per $\mu$l cell $H_2O$) | $r_{y,\hat{y}}$ | $K^{ee}$ ($\mu$M) | $V^{ee}$ (pmol/s per $\mu$l cell $H_2O$) | $r_{y,\hat{y}}$ |
| 1→2 | 1 | 509±18 | 117±1.4 | 0.996 | 881±109 | 109±8.8 | 0.993 |
| | 2 | 595±21 | 58±0.8 | 0.996 | 551± 85 | 68±5.4 | 0.993 |
| | 3 | 588±35 | 67±1.4 | 0.984 | | | |
| | 4 | 454±82 | 76±7.6 | 0.989 | | | |
| | 5 | 295±27 | 61±2.0 | 0.963 | 331± 70 | 82±4.5 | 0.978 |
| | 6 | 734±97 | 107±5.0 | 0.963 | 563± 91 | 140±7 | 0.989 |
| | 7 | 391±45 | 154±7.0 | 0.976 | | | |
| | 8 | 495±53 | 96±3.6 | 0.964 | 424±117 | 82±5 | 0.978 |
| 2→1 | 9 | | | | 636± 78 | 92±7 | 0.997 |
| Average (±S.E.) | | 508±48 | | | 564± 77 | | |

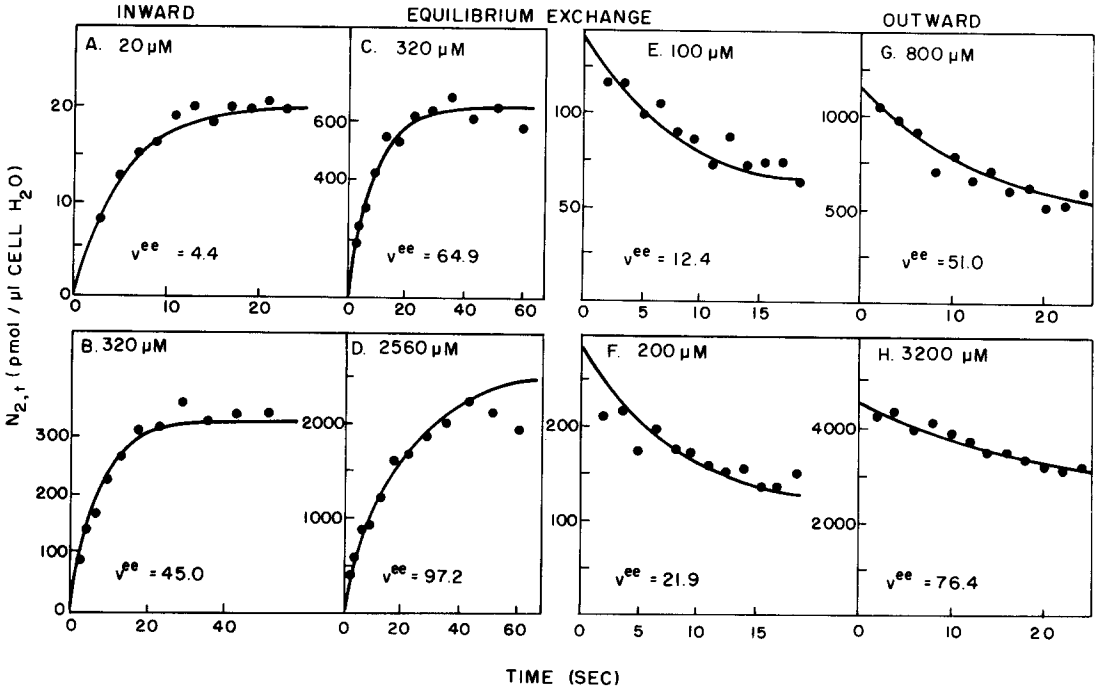


Fig. 3. Representative time courses of inward (A–D) and outward (E–H) equilibrium exchange of hypoxanthine in hypoxanthine-guanine phosphoribosyltransferase-deficient Novikoff cells at 25°C. The data are from experiments 1 and 9 in Table I, which lists the best fitting kinetic parameters obtained by fitting the appropriate integrated rate equations to the complete data sets. The initial velocities (in pmol/s per μl cell $H_2O$) were calculated from the estimated values of $K^{ee}$ and $V^{ee}$ for the given substrate concentrations as slopes of the theoretical curves at $t = 0$.

low). Differential mobilities of empty and loaded carrier are most clearly detectable by a difference between $v^{zt}$ and $v^{ee}$ when $S \gg K$ [4], whereas the two velocities approach identity when $S \ll K$ [4]. The time courses for zero-*trans* accumulation and inward equilibrium exchange of 2 mM hypoxanthine differed greatly (Fig. 1B), and might seem to suggest a difference in initial rates. But this difference is entirely predictable from Eqns. 1 and 2, based on the simple carrier model. In fact, the time courses of [$^3$H]hypoxanthine accumulation in the zero-*trans* and equilibrium exchange mode correlated very well with those simulated by computer for a simple carrier with directional symmetry, equal mobility when loaded or empty and with kinetic parameters equal to those measured for the hypoxanthine transporter (compare Fig. 1B with Fig. 2D). Graphical estimation of initial velocities from such time courses (or fitting quadratic or exponential equations) would have led to the erroneous conclusion that $v^{ee} > v^{zt}$, indicative of *trans*-stimulation, whereas integrated rate analysis clearly indicates that the two did not differ significantly. On the other hand, the time courses of 20 μM [$^3$H]hypoxanthine accumulation were about the same for zero-*trans* entry and inward equi-

Fig. 4. Examination of residuals from computer fits of Equations 1, 2 and 3 to zero-*trans*, and inward and outward equilibrium exchange data from experiments 1 and 9 (Table I), respectively. The observed and computed values of the dependent variable ($S_{2,t}$ or $N_{2,t}$) were normalized to the computed asymptotic values and are designated $y$ and $\hat{y}$, respectively. In panels A, E and I, $y - \hat{y}$ is plotted against $\hat{y}$; the different letters used as plot symbols identify the various concentrations of substrate comprising each data set in experiments 1 and 9 (with A representing the lowest concentration). In panels B, C, F, G, J and K, $y - \hat{y}$ is plotted against the independent variables ($S_1$ or $S$ and $t$). In panels D, H and L the residuals are ranked and plotted on a normal grid. In this presentation a normal distribution approaches a straight line through the origin [13,14].

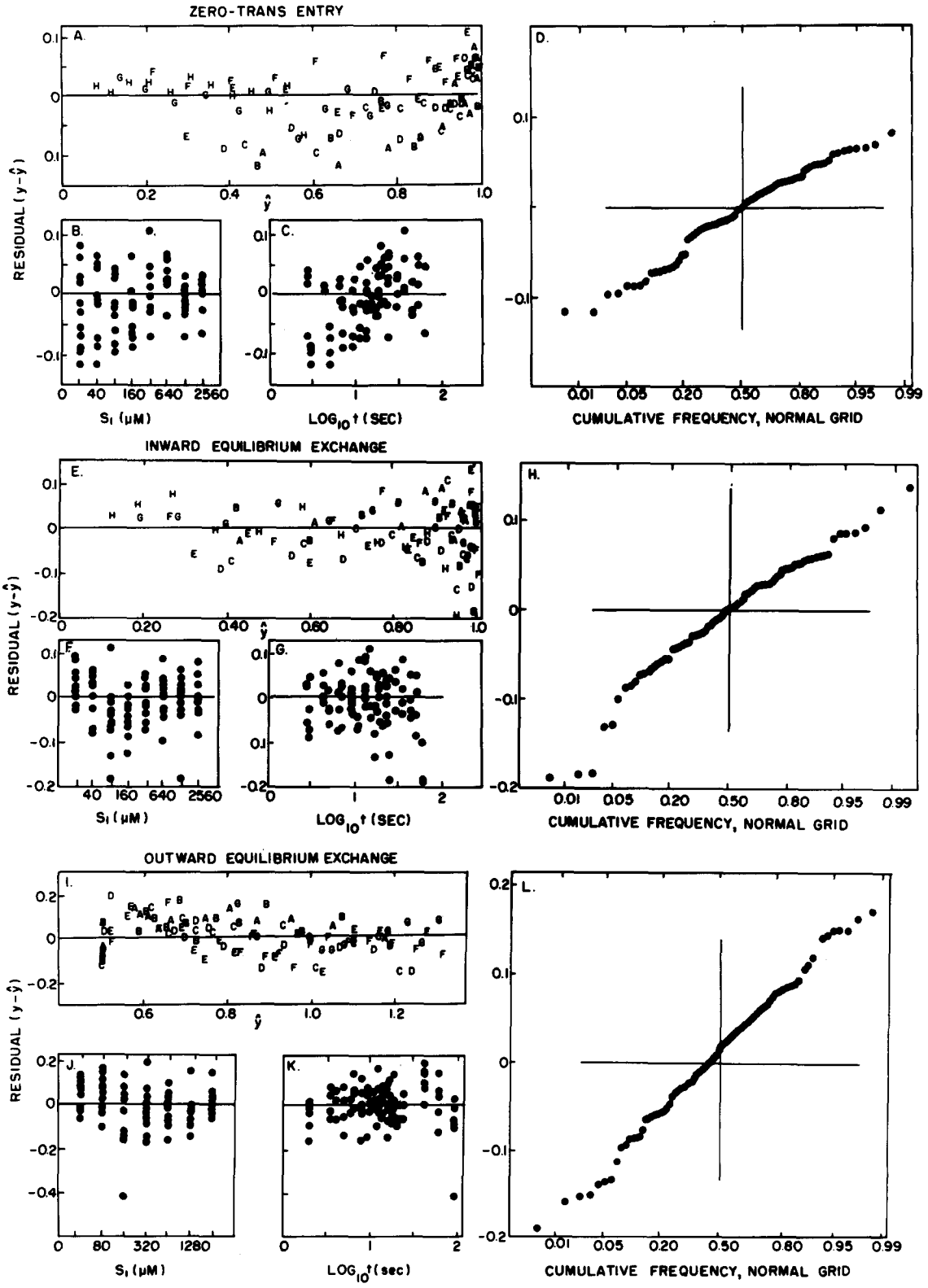
ZERO-TRANS ENTRY
A.
B.
C.
D.
RESIDUAL (y-ŷ)
ŷ
Sᵢ (μM)
LOG₁₀ t (SEC)
CUMULATIVE FREQUENCY, NORMAL GRID
INWARD EQUILIBRIUM EXCHANGE
E.
F.
G.
H.
OUTWARD EQUILIBRIUM EXCHANGE
I.
J.
K.
L.
LOG₁₀t (sec)

librium exchange, just as expected from computer simulations (compare Figs. 1A and 2A). These results emphasize the importance of applying integrated rate analysis to estimate initial transport velocities from time courses of substrate transmembrane equilibration.

Table I summarizes the kinetic parameters for zero-*trans* entry and inward and outward equilibrium exchange observed in a number of independent experiments with transferase-deficient Novikoff cells. In each experiment the appropriate integrated rate equation was fitted to data pooled for at least seven hypoxanthine concentrations (generally from 40 to 2560 $\mu$M), each time course consisting of 15 time points. Representative time courses for inward and outward equilibrium exchange are illustrated in Fig. 3; typical time courses for zero-*trans* accumulation of hypoxanthine have been presented previously [1]. The kinetic parameters for equilibrium exchange ($K^{ee}$ and $V^{ee}$) did not differ significantly from $K$ and $V$, respectively, estimated from the zero-*trans* data by assuming directional symmetry and equal mobility of loaded and empty carrier. This justifies our approach of fitting the simplified zero-*trans* equation (Eqn. 1) to the zero-*trans* entry data.

The values of $K$ and $V$ obtained in the present set of experiments are somewhat higher than those obtained in five other experiments conducted previously with transferase-deficient and ATP-depleted wild type Novikoff cells [1,3]. The reasons for this difference are not apparent. However, recently we have been propagating the cells in a somewhat modified medium (see Materials and Methods) and the medium has been supplemented with a different batch of calf serum.

We have assessed the closeness of fit of the theoretical equations to our experimental data using a number of statistical procedures [13]. The correlation coefficient, $r_{y,\hat{y}}$ (the slope of the linear regression of a plot of $y$, the experimental value (in our case, $S_{2,t}$ or $N_{2,t}$) versus $\hat{y}$, the computed theoretical value), seems to be as good an indicator of closeness of fit as any other single value, and the appropriate values of this coefficient are listed for each experiment. However, we have also routinely examined the deviations of observed ($y$) from computed values ($\hat{y}$) for tendential changes with either independent variable (i.e. with $S_1$ and $t$), or with $\hat{y}$, and have ascertained the normalcy of the overall distribution of these deviations [13]. Fig. 4 shows examples of these analyses for zero-*trans* entry, and inward and outward equilibrium exchange; the deviations, $y - \hat{y}$, were normalized to $S_{2,\infty}$ or $N_{2,\infty}$, because it is this normalized deviation squared, which the fitting program seeks to minimize. In all three cases the deivations appear to be distributed randomly around $\hat{y}$ (Figs. 4 A, E and I) and to show no bias with respect to $S$ or $t$ (Figs. 4 B, C, F, G, J and K). The normalcy of the distributions of the deviations overall are demonstrated in Figs. 4 D, H and L by their falling on a straight line through the origin of the grid. These plots are best appreciated in comparison with similar plots of samples from authentic, normally distributed populations as presented by Daniel and Wood [14]. None of these statistical procedures, of course, proves that the fitted equations are the correct ones, but they indicate nevertheless, that the experimental time courses of hypoxanthine transmembrane equilibration both in the zero-*trans* and equilibrium exchange modes are well described by the appropriate equations derived from the simple carrier model.

In its directional symmetry and equal mobility of empty and substrate-loaded carrier, the hypoxanthine transporter is identical to the nucleoside transporter (Refs. 3 and 18, and Wohlhueter, R.M., Erbe, J. and Plagemann, P.G.W., unpublished data), but both differ in one of these properties from the hexose transporter of cultured mammalian cells. The hexose transporter is also symmetrical with respect to direction, but it moves more rapidly when loaded than when empty [4,15]. Work with the hexose transporter showed that a 2-fold differential mobility of loaded and empty carrier can readily be detected by our procedures. Nucleoside and hypoxanthine transport exhibit other overlapping features; for example, their kinetic parameters are similar, the transport of nucleosides is inhibited by hypoxanthine, and the transport of hypoxanthine is inhibited by various nucleosides [3]. They are, however, distinguishable genetically and on the basis of their sensitivity to inhibition by nitrobenzylthioinosine (6-((4-nitrobenzyl)thio)-9-$\beta$-D-ribofuranosylpurine). Nucleoside transport in Chinese hamster ovarian cells is strongly inhibited by nitrobenzylthioinosine ($K_i \sim$

1 nM), whereas hypoxanthine transport is little affected by a concentration of the analog which inhibits nucleoside transport about 90% [16]. Also, a mutant of the mouse T-cell line S49 which is defective in the uptake of various nucleosides (strain AE1) takes up hypoxanthine unabated [17]. Thus, further work is required to assess the relationship between nucleoside and hypoxanthine transport.

*Estimation of kinetic parameters for hypoxanthine transport from uptake curves with wild type cells*

We have also determined whether the kinetic parameters for hypoxanthine transport can be deduced from time-courses of zero-*trans* hypoxanthine uptake by wild-type Novikoff cells in which hypoxanthine is phosphoribosylated. Fig. 5 illustrates early time courses of uptake at hypoxanthine concentrations from 40 to 2560 $\mu$M. From replicate cell samples we extracted the acid-soluble pools and used chromatographic analysis to quantitate the amount of radioactivity in phosphorylated products. When the hypoxanthine concentration was 40 $\mu$M (Fig. 5A), uptake was approximately linear and the intracellular concentration of radioactivity exceeded that in the medium within 10 s of incubation. The data are in agreement with previously reported results [1]. Within a few seconds free hypoxanthine attained an intracellular steady-state level of about 80% of that in the medium and uptake reflected the accumulation of labeled nucleotides. After 60 s of incubation 50% of the intracellular radioactivity was associated with nucleotides (data not shown). The hypoxanthine phosphoribosyltransferase ($K_m$ = 2–6 $\mu$M [1]), therefore, became rapidly saturated at this and higher hypoxanthine concentrations and with increase in hypoxanthine concentration, a progressively smaller proportion of the entering hypoxanthine became phosphoribosylated, until at a concentration of 2560 $\mu$M only about 5% of the intracellular radioactivity was associated with nucleotides after 60 s of incubation. Thus at higher concentrations the rate of phosphoribosylation was insignificant in comparison to the rate of hypoxanthine entry, and the time-courses of hypoxanthine uptake largely reflected the accumulation of unmodified substrate. This is borne out by the fits of Eqn. 1 to the data. Curves drawn according to the kinetic parameters obtained by fitting all the data coincide reasonably well with the data at concentrations above 160 $\mu$M, and the estimated kinetic parameters were similar to those obtained with cells deficient in phosphoribosylation. We fitted Eqn. 1 to increasingly smaller sets of data by omitting one concentration at a time beginning with 40 $\mu$M (see values in inset of Fig. 5). Little improvement in fit was statistically evident since decreasing deviations were offset by smaller numbers of data, although slightly higher $K$ values were obtained by omitting the lower concentrations. The analyses show that the kinetic parameters for substrate transport can be approximated

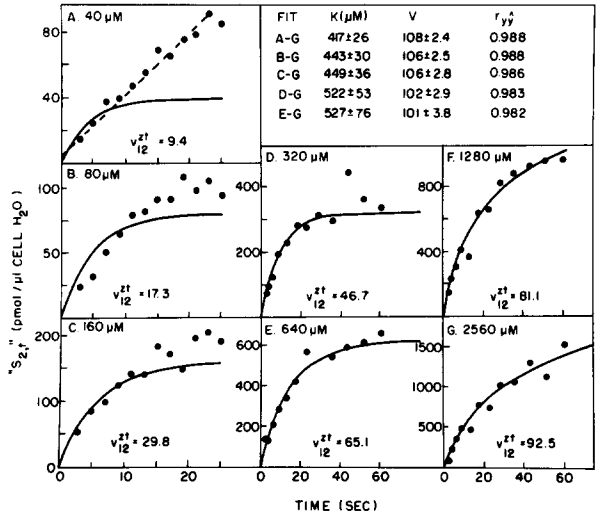


Fig. 5. Fits of Eqn. 1 to time-courses of zero-*trans* uptake of [$^3$H]hypoxanthine by wild type Novikoff cells at 25°C. The uptake of the various concentrations of [$^3$H]hypoxanthine (600 cpm/$\mu$l, regardless of concentration) was measured by the rapid kinetic technique. All radioactivity values were corrected for substrate trapped in extracellular space (2.5 $\mu$l/509 $\mu$l sample of cell suspension) and converted to pmol/$\mu$l cell $H_2O$ on the basis of an intracellular $H_2O$ space of 15 $\mu$l per sample. Eqn. 1 was fitted in turn to the data pooled for panels A–G, B–G, C–G, D–G and E–G and the best fitting kinetic parameters (±S.E. of estimate) are listed in the inset. (See text for the rationale of progressively excluding low concentrations of exogenous hypoxanthine from the kinetic analyses.) The theoretical curves shown are those resulting from fitting Eqn. 1 to the complete data set (A–G). $S_{2,t}$ is set in quotations to indicate that the measurement includes all radioactivity derived from hypoxanthine, and is not strictly the chemical concentration of hypoxanthine. Initial velocities (in pmol/$\mu$l cell $H_2O$) were calculated from the estimated values of $K$ and $V$ for a given substrate concentration as the slopes of the theoretical curves at $t = 0$.

with reasonable accuracy from time-courses of substrate uptake if analysis is confined to time intervals at which intracellular concentrations of isotope remain substantially less than that in the extracellular fluid. This condition is readily met if the Michaelis-Menten constant and maximum velocity for transport are two orders of magnitude higher than those for the enzyme that is rate-determining in its conversion to phosphorylated products as is the case for hypoxanthine [1].

## Acknowledgements

We thank John Erbe, Patricia Wilkie, Karen Wittkop and Laurie Peterson for excellent technical assistance and Colleen O'Neill for competently typing the manuscript. This work was supported by USPHS Research Grant GM 24468.

## References

1 Marz, R., Wohlhueter, R.M. and Plagemann, P.G.W. (1979) J. Biol. Chem. 254, 2329–2338
2 Eilam, Y. and Stein, W.D. (1974) Methods Membrane Biol. 2, 283–354
3 Plagemann, P.G.W. and Wohlhueter, R.M. (1980) Curr. Top. Membrane Transp. 14, 225–330
4 Graff, J.D., Wohlhueter, R.M. and Plagemann, P.G.W. (1981) Biochim. Biophys. Acta 641, 320–333
5 Zylka, J.M. and Plagemann, P.G.W. (1975) J. Biol. Chem. 250, 5756–5767
6 Plagemann, P.G.W. and Swim, H.E. (1966) J. Bacteriol. 91, 2317–2326
7 Schneider, E.L., Stanbridge, E.F. and Epstein, C.J. (1974) Exp. Cell. Res. 84, 311–318
8 Kenny, G.E. (1973) in Contamination in Tissue Culture (Fogh, J., ed.), pp. 107–129, Academic Press, New York
9 Plagemann, P.G.W. (1971) J. Cell. Physiol. 77, 213–240
10 Wohlhueter, R.M., Marz, R., Graff, J.C. and Plagemann, P.G.W. (1978) Methods Cell Biol. 16, 211–236
11 Wohlhueter, R.M., Marz, R. and Plagemann, P.G.W. (1979) Biochim. Biophys. Acta 553, 262–283
12 Dietrich, O.W. and Rothmann, O.S. (1975) Keyboard 7, 4–6
13 Draper, N.R. and Smith, H. (1966) Applied Regression Analysis, John Wiley and Sons, New York
14 Daniel, C. and Wood, F.S. (1971) Fitting Equations to Data, Chap. 3, Wiley-Interscience, New York
15 Plagemann, P.G.W., Wohlhueter, R.M., Graff, J., Erbe, J. and Wilkie, P. (1981) J. Biol. Chem. 256, 2835–2842
16 Wohlhueter, R.M., Marz, R. and Plagemann, P.G.W. (1978) J. Membrane Biol. 42, 247–264
17 Cohen, A., Ullman, B. and Martin, D.W., Jr. (1979) J. Biol. Chem. 254, 112–118
18 Wohlhueter, R.M., Erbe, J. and Plagemann, P.G.W. (1980) Fed. Proc. 39, 1839